25

A Convenient and Inexpensive Quality Control Method for Examining the Accuracy of Conjugate Cam Profiles

Wen-Tung Chang[1] and Long-Iong Wu[2]
[1]*Opto-Mechatronics Technology Center, National Taiwan University of Science and Technology, Taipei 10607*
[2]*Department of Power Mechanical Engineering, National Tsing Hua University, Hsinchu 30013 Taiwan*

1. Introduction

The cam mechanism, basically consisting of a frame, a cam and a translating or oscillating follower with a roller in contact with the cam, is a simple and reliable device for motion control in machinery. Being a high-value-added product, a conjugate cam mechanism consists of a pair of disk cams that their profiles must be mutually conjugate to contact their respective follower. The conjugate cam mechanism is therefore a positive-drive mechanism (Wu, 2003; Rothbart, 2004; Norton, 2009) that can eliminate the use of return springs. As a benefit of positive-drive, the conjugate cam mechanism can ensure the contact between the cam and the follower roller with lower contact stresses between them. Such a situation can further contribute to the reduction of excessive noise, wear and vibrations occurred in the mechanism. In other words, reasonably designed conjugate cam mechanisms are especially suited to high-speed applications. However, since a conjugate cam mechanism is a so-called kinematically overconstrained arrangement (Wu, 2003), to ensure its movability condition and its ability to run without backlash (Rothbart, 2004; Norton, 2009), its cam profiles must be accurately designed and machined. The machined cams must then be carefully examined to check whether their profile errors fall within a specified tolerance range in order to achieve high quality and performance of the mechanism.

Up to the present time, using a highly sensitive and accurate coordinate measuring machine (CMM) to examine the accuracy of machined cam profiles is an industry-recognized technique, although it is still costly and time-consuming. For the quality control of machined cams, the cam profile must be directly measured by using a CMM, while the path planning and/or the coordinate measuring data are dealt with by some mathematical approaches to evaluate the profile errors (Lin & Hsieh, 2000; Qiu et al., 2000a; Qiu et al., 2000b; Qiu et al., 2000c; Hsieh & Lin, 2007; Chang et al., 2008). As an alternative quality control method, a special conjugation measuring fixture, which is improved from the one proposed by Koloc and Václavík (1993) and further investigated by Chang and Wu (2008), is developed by Chang et al. (2009) for indirectly evaluating the profile errors of conjugate disk cams. The conjugation measuring fixtures are based on the means of measuring the conjugate variation

of the assembled conjugate cam mechanism. According to the concept proposed by Chang et al. (2009), for a conjugate cam mechanism with an oscillating roller follower as shown in Fig. 1, if the constant center distance between the cam and follower pivots, f, is intentionally changed to be a variable parameter, f^*, by enabling the follower (link 3) being pivoted on a slider (link 4), as shown in Fig. 2, the mechanism will no longer be overconstrained. In other words, the follower subassembly (links 3 and 4) can serve as a conjugation measuring fixture. For the assembled conjugate cams with profile errors, the magnitude of distance f^* will vary with respect to the cam rotation angle θ, and the variation of the center distance between the cam and follower pivots, Δf ($= f^* - f$), can be detected by directly measuring the positional variation of the slider with the use of an inexpensive linear displacement meter, such as a dial (or digimatic) indicator or a linear scale, and the meter reading can indicate the variation of cam profile errors. Such a measurement method should be more convenient and inexpensive than the use of a CMM. By applying this concept, Chang et al. (2009) have presented a rapid indirect method for examining profile deviations of conjugate disk cams. In their work, an analytical approach called conjugate variation analysis (or conjugate condition analysis), based on the mechanical error analysis of disk cam mechanisms (Wu and Chang, 2005; Chang and Wu, 2006), has been developed for relating the center distance variation with the profile deviations of a pair of conjugate disk cams. Then, conservative criteria for qualify control of assembled conjugate cams with the measurement of the center distance variation have been proposed and an experimental verification had also been conducted. However, the rapid indirect method itself is mainly applied for evaluating whether the conjugate variation induced by a pair of machined conjugate disk cams is acceptable, but not able to examine the profile errors of each individual machined cam.

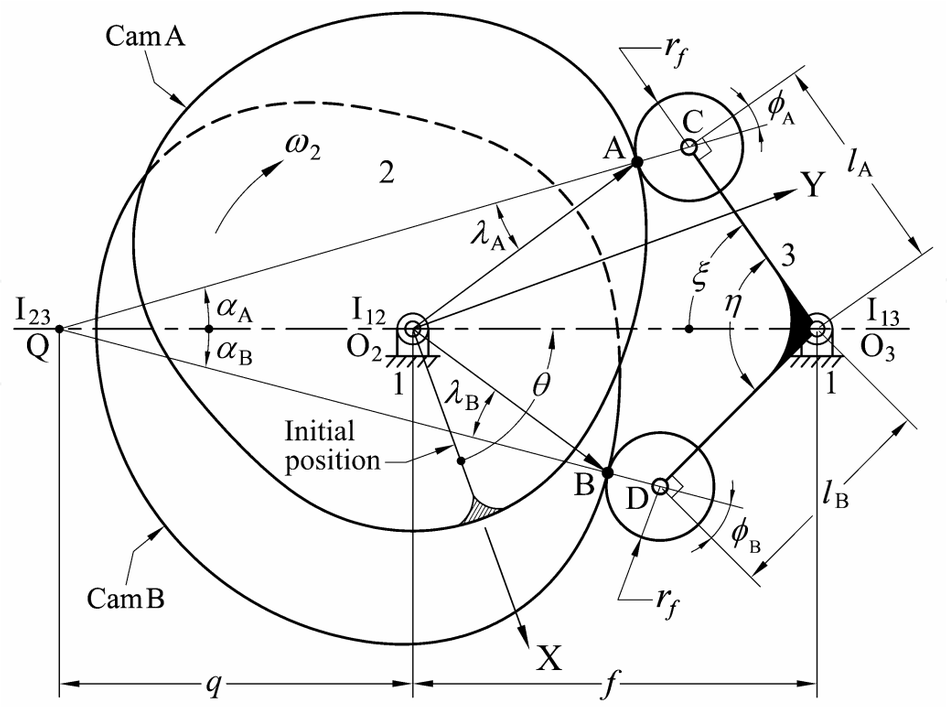

Fig. 1. Conjugate disk cams with an oscillating roller follower

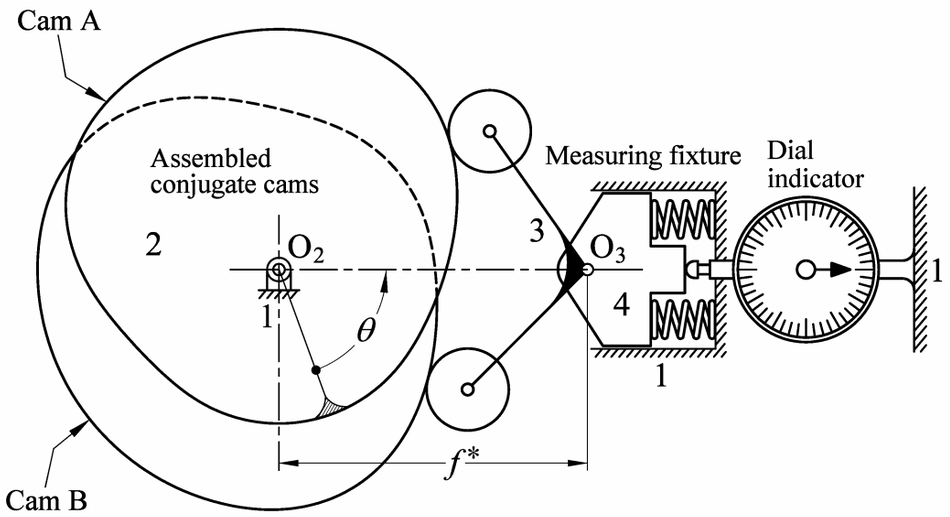

Fig. 2. Assembled conjugate cams with measuring fixture

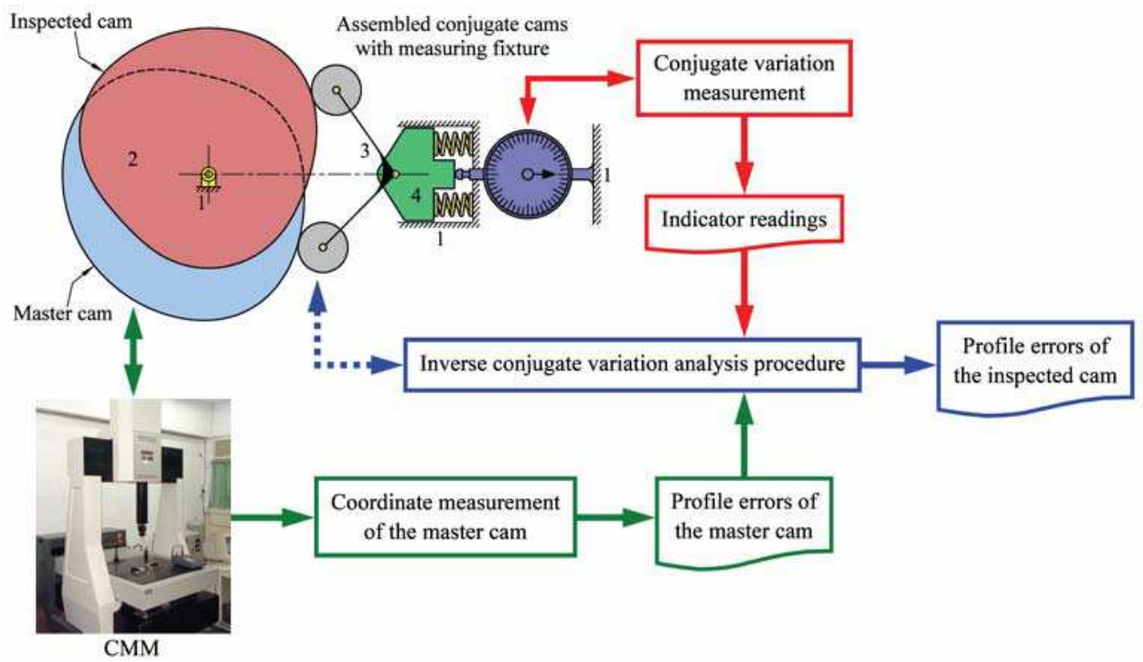

Fig. 3. Procedure for profile error estimation of the inspected cam

From the practical perspective of cam design and manufacture, a pair of conjugate disk cams can be machined in one piece or each cam be machined individually and then assembled together. The latter is usually a relatively easy and inexpensive manner, especially for mass production of conjugate cams. When the design of assembled conjugate cams is adopted, based on the concept of the rapid indirect method (Chang et al., 2009), an improved manner for examining the profile errors of each individual machined cam can be further developed. That is, if a pair of master conjugate cams with known profile errors is additionally available, through the measured center distance variations induced by a pair of

assembled conjugate cams that consists of one master cam and the other being the inspected cam, then the profile errors of each inspected cam can be estimated and examined. Such a concept is abstractly shown in Fig. 3; in which, for a pair of assembled conjugate cams consisting of one master cam, whose profile errors have been measured by using a CMM, and the other being the inspected cam, through the measurement of the center distance variation and the "inverse conjugate variation analysis procedure" of the assembled conjugate cam mechanism, the profile errors of the inspected cam can be estimated and then examined by an analytical manner. For the quality control in mass production of assembled conjugate disk cams, simply a pair of master conjugate cams with known profile errors and a set of conjugation measuring fixture must be prepared.

The objective of this study is to demonstrate how to examine the profile accuracy of assembled conjugate disk cams by applying the conjugate variation measurement and the inverse conjugate variation analysis. In order to verify the feasibility of the presented concept, an experiment meant to examine profile errors of a pair of machined conjugate cams was conducted. The profile errors of the machined cams estimated by using the presented method were compared with the measuring results obtained by using a CMM.

2. Parametric expressions for the conjugate cam profiles

In order to evaluate the dimensional variations of the machined cam profiles, the analytical expressions for the theoretical cam profiles must be derived first. For easy reference, the analytical expressions derived by Wu (2003) are provided in this section. For the conjugate cam mechanism shown in Fig. 1, its two cams A and B are fixed on a common shaft. Its two follower rollers C and D, mounted to a common follower, are each pushed in opposite directions by the conjugate cams. In the figure, f represents the distance from the cam center O_2 to the follower pivot point O_3, r_f represents the radii of rollers C and D, l_A and l_B represent the arm lengths of the follower, and η is the fixed subtending angle of the follower arms. By setting up a Cartesian coordinate system X-Y fixed on the cam and with its origin at the fixed pivot O_2, the cam profile coordinates may be expressed in terms of θ, which is measured against the direction of cam rotation from the reference radial on cam to the line of centers (line O_2O_3). In order to let θ have a counterclockwise angle, the cam is to rotate clockwise with a constant angular velocity of $\omega 2$.

As referred to in Fig. 1, the two normal lines through the points of contact and line of centers must always intersect at the instant center I_{23} (Wu, 2003), where "I" denotes the instant center and subscripts indicate the related links. For simplicity, in the following, the frame will be consistently numbered as 1, the cam as 2 and the follower as 3. By labeling instant center I_{23} as Q and $O_2Q = q$, the parametric vector equations of the cam profile coordinates are (Wu, 2003)

$$\mathbf{O_2A} = \begin{Bmatrix} X_A(\theta) \\ Y_A(\theta) \end{Bmatrix} = \begin{Bmatrix} (QC - r_f)\cos(\theta + \alpha_A) - q\cos\theta \\ (QC - r_f)\sin(\theta + \alpha_A) - q\sin\theta \end{Bmatrix} \tag{1}$$

$$\mathbf{O_2B} = \begin{Bmatrix} X_B(\theta) \\ Y_B(\theta) \end{Bmatrix} = \begin{Bmatrix} (QD - r_f)\cos(\theta - \alpha_B) - q\cos\theta \\ (QD - r_f)\sin(\theta - \alpha_B) - q\sin\theta \end{Bmatrix} \tag{2}$$

where

$$q = \frac{f\dfrac{d\xi(\theta)}{d\theta}}{1-\dfrac{d\xi(\theta)}{d\theta}} \tag{3}$$

$$\mathrm{QC} = \sqrt{l_{\mathrm{A}}^2 + (f+q)^2 - 2l_{\mathrm{A}}(f+q)\cos\xi(\theta)} \tag{4}$$

$$\mathrm{QD} = \sqrt{l_{\mathrm{B}}^2 + (f+q)^2 - 2l_{\mathrm{B}}(f+q)\cos[\eta-\xi(\theta)]} \tag{5}$$

$$\alpha_{\mathrm{A}} = \sin^{-1}\left[\frac{l_{\mathrm{A}}\sin\xi(\theta)}{\mathrm{QC}}\right] \tag{6}$$

$$\alpha_{\mathrm{B}} = \sin^{-1}\left\{\frac{l_{\mathrm{B}}\sin[\eta-\xi(\theta)]}{\mathrm{QD}}\right\} \tag{7}$$

in which, $\xi(\theta)$ is the angular displacement function of the follower:

$$\xi(\theta) = \cos^{-1}\left[\frac{l_{\mathrm{A}}^2 + f^2 - (r_b + r_f)^2}{2l_{\mathrm{A}}f}\right] + S(\theta) \tag{8}$$

where r_b is the radius of the base circle of cam A, and $S(\theta)$ is the follower angular motion program. Thus, in Eq. (3),

$$\frac{d\xi(\theta)}{d\theta} = \frac{dS(\theta)}{d\theta} = V(\theta) \tag{9}$$

in which, $V(\theta)$ is the follower angular velocity program. Also, the pressure angles ϕ_{A} and ϕ_{B} of the conjugate cam mechanism can be expressed as (Wu, 2003)

$$\phi_{\mathrm{A}} = 90° - \alpha_{\mathrm{A}} - \xi(\theta) \tag{10}$$

$$\phi_{\mathrm{B}} = 90° - \alpha_{\mathrm{B}} - [\eta - \xi(\theta)] \tag{11}$$

In addition, the shift angles λ_{A} and λ_{B} of the cam profiles, that is, the subtending angles between the radial and normal lines through the points of contact, can be expressed as (Chang et al., 2008; Chang & Wu, 2008; Chang et al., 2009)

$$\lambda_{\mathrm{A}} = \angle \mathrm{O_2AQ} = \sin^{-1}\left(\frac{q\sin\alpha_{\mathrm{A}}}{\|\mathbf{O_2A}\|}\right) = \sin^{-1}\left\{\frac{fV(\theta)\sin\alpha_{\mathrm{A}}}{[1-V(\theta)]\|\mathbf{O_2A}\|}\right\} \tag{12}$$

$$\lambda_{\mathrm{B}} = \angle \mathrm{O_2BQ} = \sin^{-1}\left(\frac{q\sin\alpha_{\mathrm{B}}}{\|\mathbf{O_2B}\|}\right) = \sin^{-1}\left\{\frac{fV(\theta)\sin\alpha_{\mathrm{B}}}{[1-V(\theta)]\|\mathbf{O_2B}\|}\right\} \tag{13}$$

These two angles are derived geometric parameters for correlating radial-dimension errors and normal-direction errors of disk cam profiles (Chang et al., 2008; Chang & Wu, 2008; Chang et al., 2009).

3. Conjugate variation measurement and the examination of profile accuracy

The measurement of the conjugate variation of the assembled conjugate cam mechanism can indirectly reveal the cam profile errors. By applying the analytical approach of the conjugate variation analysis (Chang et al., 2009), a convenient and inexpensive means for examining the profile accuracy of each individual machined cam can be developed.

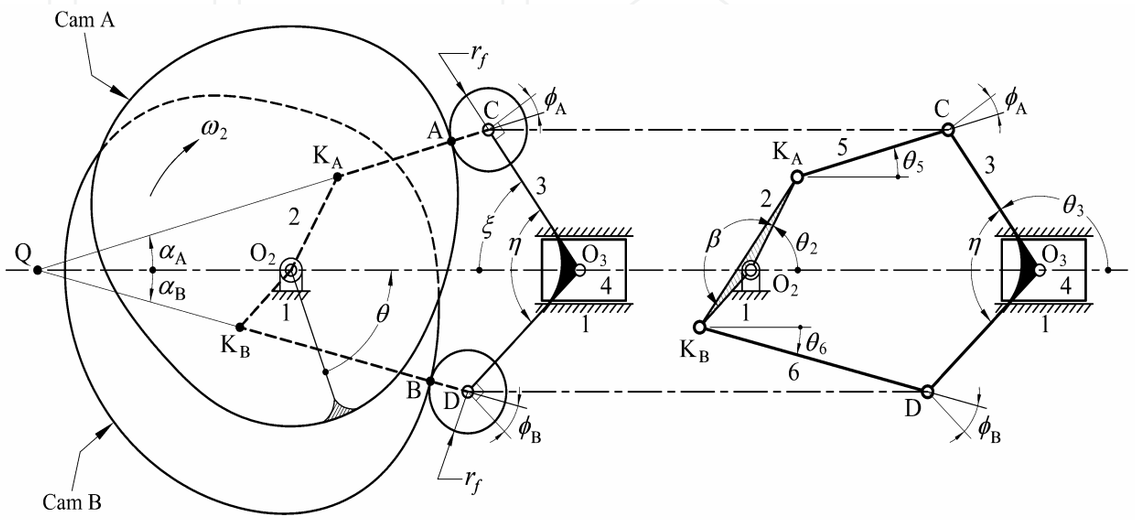

Fig. 4. An assembled conjugate cam mechanism and its equivalent six-bar linkage

3.1 Basic concepts

As referred to in Figs. 1 and 2, the center distance between the cam and follower pivots in the conjugation measuring fixture is designed to be variable. The difference between the variable center distance f^* (that is between the cam and follower pivots) and its ideally constant distance f may be induced by the radial-dimension errors of cams A and B, Δr_A and Δr_B, the roller-radius errors of rollers C and D, Δr_{fC} and Δr_{fD}, the errors of the arm lengths, Δl_A and Δl_B, and the subtending angle error of the follower arms, $\Delta\eta$. As a special case of the mechanical error analysis of disk cam mechanisms (Wu and Chang, 2005; Chang and Wu, 2006), by employing the concept of equivalent six-bar linkage of this assembled conjugate cam mechanism, as shown in Fig. 4, the analytical expressions of the center distance variations, Δf_r caused by Δr_A and Δr_B, Δf_{rf} caused by Δr_{fC} and Δr_{fD}, Δf_l caused by Δl_A and Δl_B, and Δf_η caused by $\Delta\eta$, respectively, have been derived as (Chang et al., 2009)

$$\Delta f_r \approx \frac{\Delta r_A (l_B \cos\phi_B \cos\lambda_A) + \Delta r_B (l_A \cos\phi_A \cos\lambda_B)}{l_A \cos\phi_A \cos\alpha_B + l_B \cos\phi_B \cos\alpha_A} \tag{14}$$

$$\Delta f_{rf} = \frac{\Delta r_{fC} (l_B \cos\phi_B) + \Delta r_{fD} (l_A \cos\phi_A)}{l_A \cos\phi_A \cos\alpha_B + l_B \cos\phi_B \cos\alpha_A} \tag{15}$$

$$\Delta f_l = \frac{\Delta l_A (l_B \cos\phi_B \sin\phi_A) + \Delta l_B (l_A \cos\phi_A \sin\phi_B)}{l_A \cos\phi_A \cos\alpha_B + l_B \cos\phi_B \cos\alpha_A} \tag{16}$$

$$\Delta f_\eta = -\frac{\Delta\eta(l_A l_B \cos\phi_A \cos\phi_B)}{l_A \cos\phi_A \cos\alpha_B + l_B \cos\phi_B \cos\alpha_A} \tag{17}$$

in which, the correlations of $\theta_5 = \alpha_A$ and $\theta_6 = \alpha_B$ exist as shown in Fig. 4. Also, parameters θ_2 and β depending on the locations of points K_A and K_B, which are the centers of curvatures of cams A and B respectively, are not involved in the derived results of Eqs. (14)-(17). Note that in practice, depending on the value of cam rotation angle θ, the magnitudes of the cam profile errors Δr_A and Δr_B may vary, while Δr_{fC}, Δr_{fD}, Δl_A, Δl_B and $\Delta\eta$ remain constant. In other words, $\Delta r_A = \Delta r_A(\theta)$ and $\Delta r_B = \Delta r_B(\theta)$. Assuming the small manufacturing or assembly errors $\Delta r_A(\theta)$, $\Delta r_B(\theta)$, Δr_{fC}, Δr_{fD}, Δl_A, Δl_B and $\Delta\eta$ in the assembled conjugate cam mechanism have been precisely measured, the overall center distance variation can be approximated by the sum of the derived center distance variations:

$$\Delta f_{est} = \Delta f_r + \Delta f_{rf} + \Delta f_l + \Delta f_\eta \tag{18}$$

Ideally, the estimated variation Δf_{est} will be equal to the measured value Δf_{mea} that can be obtained by means of a dial indicator as shown in Fig. 2. In the following context, the subscript "est" indicates estimated or calculated terms, while the subscript "mea" indicates actually measured ones.

The measurement of the center distance variation can be inversely applied to develop a convenient and inexpensive means for examining the conjugate cam profile errors. From Eq. (18) and considering the correlation of $\Delta f_{mea} \approx \Delta f_{est}$, it follows that

$$\Delta f_r \approx \Delta f_{mea} - (\Delta f_{rf} + \Delta f_l + \Delta f_\eta) \tag{19}$$

If the error terms Δr_{fC}, Δr_{fD}, Δl_A, Δl_B, $\Delta\eta$ and Δf_{mea} have been precisely measured and then Δf_{rf}, Δf_l and Δf_η have been evaluated by using Eqs. (15)-(17), respectively, Eq. (19) itself can accurately predict the center distance variation Δf_r without knowing the actual cam profile errors Δr_A and Δr_B. In order to calculate the unknown cam profile error Δr_A, however, the radial profile error of cam B must be measured in advance. From Eqs. (14) and (19), the estimated (calculated) radial profile error of cam A will be

$$\Delta r_{A,est} \approx \frac{1}{l_B \cos\phi_B \cos\lambda_A}\Big\{(l_A \cos\phi_A \cos\alpha_B + l_B \cos\phi_B \cos\alpha_A)[\Delta f_{mea} - (\Delta f_{rf} + \Delta f_l + \Delta f_\eta)] - \Delta r_{B,mea}(l_A \cos\phi_A \cos\lambda_B)\Big\} \tag{20}$$

where $\Delta r_{B,mea}$ is the measured radial profile error of cam B. Likewise, if the radial profile error of cam A has been measured, the unknown cam profile error Δr_B can be estimated (calculated) by

$$\Delta r_{B,est} \approx \frac{1}{l_A \cos\phi_A \cos\lambda_B}\Big\{(l_A \cos\phi_A \cos\alpha_B + l_B \cos\phi_B \cos\alpha_A)[\Delta f_{mea} - (\Delta f_{rf} + \Delta f_l + \Delta f_\eta)] - \Delta r_{A,mea}(l_B \cos\phi_B \cos\lambda_A)\Big\} \tag{21}$$

where $\Delta r_{A,mea}$ is the measured radial profile error of cam A. In order to proceed with such a cam profile error estimation, it is necessary to have two master cams $A_{(m)}$ and $B_{(m)}$ whose profiles are precisely measured and thus the magnitudes of $\Delta r_{A,mea}$ and $\Delta r_{B,mea}$ in the above

two equations, respectively, can be known. Then, for a conjugate cam mechanism, the profile errors of each cam can be estimated subsequently by means of the conjugate variation measurement. The process presented above can be regarded as the "inverse conjugate variation analysis procedure" of the assembled conjugate cam mechanism.

As referred to in Fig. 3, for good cam profile control in mass production of conjugate cams, one must prepare a pair of master cams $A_{(m)}$ and $B_{(m)}$ whose profiles are accurately machined and also precisely measured by using a CMM to obtain each of their small cam profile errors. Then, if the finished products of cam A are to be examined, the inspected cam A and the master cam $B_{(m)}$ are mounted together as a pair to be measured. Once the center distance variations induced by this pair of cams have been measured, the actual profile of the inspected cam A can be estimated by means of the above presented inverse conjugate variation analysis procedure. On the other hand, if the finished products of cam B are to be examined, the inspected cam B and the master cam $A_{(m)}$ must be mounted together as a pair to be measured.

Based on the presented concept, criteria for determining whether the machined cam profiles are qualified can be established as follows. For the examination of cam A, after its upper and lower bounds of the radial-dimension errors, $\Delta r_{A(u)}$ and $\Delta r_{A(l)}$, are specified, the upper and lower acceptable extreme deviations of the center distance will be

$$\Delta f_{A(u),\text{est}} = \Delta f_{r,A(u)} + \Delta f_{rf} + \Delta f_l + \Delta f_\eta \tag{22}$$

and

$$\Delta f_{A(l),\text{est}} = \Delta f_{r,A(l)} + \Delta f_{rf} + \Delta f_l + \Delta f_\eta \tag{23}$$

in which,

$$\Delta f_{r,A(u)} \approx \frac{\Delta r_{A(u)}(l_B \cos\phi_B \cos\lambda_A) + \Delta r_{B(m),\text{mea}}(l_A \cos\phi_A \cos\lambda_B)}{l_A \cos\phi_A \cos\alpha_B + l_B \cos\phi_B \cos\alpha_A} \tag{24}$$

and

$$\Delta f_{r,A(l)} \approx \frac{\Delta r_{A(l)}(l_B \cos\phi_B \cos\lambda_A) + \Delta r_{B(m),\text{mea}}(l_A \cos\phi_A \cos\lambda_B)}{l_A \cos\phi_A \cos\alpha_B + l_B \cos\phi_B \cos\alpha_A} \tag{25}$$

where $\Delta r_{B(m),\text{mea}}$ is the known radial-dimension error of the master cam $B_{(m)}$. Then, the necessary condition of a qualified cam A is

$$\Delta f_{A(l),\text{est}} \le \Delta f_{\text{mea}} \le \Delta f_{A(u),\text{est}} \tag{26}$$

That is, if the profile deviation of an inspected cam A falls within its specified tolerance range, the measured value of the center distance variation, Δf_{mea}, will also fall within the range of $\Delta f_{A(l),\text{est}} \sim \Delta f_{A(u),\text{est}}$. Likewise, for the examination of cam B, after its upper and lower bounds of the radial-dimension errors, $\Delta r_{B(u)}$ and $\Delta r_{B(l)}$, are specified, the upper and lower acceptable extreme deviations of the center distance will be

$$\Delta f_{B(u),\text{est}} = \Delta f_{r,B(u)} + \Delta f_{rf} + \Delta f_l + \Delta f_\eta \tag{27}$$

and

$$\Delta f_{\mathrm{B}(l),\mathrm{est}} = \Delta f_{r,\mathrm{B}(l)} + \Delta f_{rf} + \Delta f_{l} + \Delta f_{\eta} \tag{28}$$

in which,

$$\Delta f_{r,\mathrm{B}(u)} \approx \frac{\Delta r_{\mathrm{A}(m),\mathrm{mea}}(l_{\mathrm{B}}\cos\phi_{\mathrm{B}}\cos\lambda_{\mathrm{A}}) + \Delta r_{\mathrm{B}(u)}(l_{\mathrm{A}}\cos\phi_{\mathrm{A}}\cos\lambda_{\mathrm{B}})}{l_{\mathrm{A}}\cos\phi_{\mathrm{A}}\cos\alpha_{\mathrm{B}} + l_{\mathrm{B}}\cos\phi_{\mathrm{B}}\cos\alpha_{\mathrm{A}}} \tag{29}$$

and

$$\Delta f_{r,\mathrm{B}(l)} \approx \frac{\Delta r_{\mathrm{A}(m),\mathrm{mea}}(l_{\mathrm{B}}\cos\phi_{\mathrm{B}}\cos\lambda_{\mathrm{A}}) + \Delta r_{\mathrm{B}(l)}(l_{\mathrm{A}}\cos\phi_{\mathrm{A}}\cos\lambda_{\mathrm{B}})}{l_{\mathrm{A}}\cos\phi_{\mathrm{A}}\cos\alpha_{\mathrm{B}} + l_{\mathrm{B}}\cos\phi_{\mathrm{B}}\cos\alpha_{\mathrm{A}}} \tag{30}$$

where $\Delta r_{\mathrm{A}(m),\mathrm{mea}}$ is the known radial-dimension error of the master cam $\mathrm{A}_{(m)}$. Then, the necessary condition of a qualified cam B is

$$\Delta f_{\mathrm{B}(l),\mathrm{est}} \le \Delta f_{\mathrm{mea}} \le \Delta f_{\mathrm{B}(u),\mathrm{est}} \tag{31}$$

When the profile deviation of an inspected cam B falls within its specified tolerance range, the measured value of the center distance variation, Δf_{mea}, will also fall within the range of $\Delta f_{\mathrm{B}(l),\mathrm{est}} \sim \Delta f_{\mathrm{B}(u),\mathrm{est}}$. Because $\Delta f_{\mathrm{A}(u),\mathrm{est}}$, $\Delta f_{\mathrm{A}(l),\mathrm{est}}$, $\Delta f_{\mathrm{B}(u),\mathrm{est}}$ and $\Delta f_{\mathrm{B}(l),\mathrm{est}}$ will vary with respect to the cam rotation angle θ, their corresponding values should be calculated for the cam profile examination.

3.2 Simulated example

The presented method will be illustrated by the following simulated example.

A conjugate cam system requires the oscillating roller follower to oscillate 30° clockwise with cycloidal motion (Rothbart, 2004; Norton, 2009) while the cam rotates clockwise from 0° to 120°, dwell for the next 40°, return with cycloidal motion for 120° cam rotation and dwell for the remaining 80°. The distance between pivots, f, is 120 mm. The lengths of the follower arms, l_{A} and l_{B}, are both equal to 66 mm, and both follower rollers have the same radius of 16 mm. The base circle radius, r_b, is 60 mm and the theoretical subtending angle of the follower arms, η, is 100°.

The profiles of cams A and B, with respective maximum radial dimensions of 93.793 mm and 93.859 mm, are shown in Fig. 1. For a tolerance grade of IT6, the cam profiles may have tolerance amounts of $\pm\Delta r_{\mathrm{A}} = \pm\Delta r_{\mathrm{B}} = \pm 22$ μm (i.e., $\Delta r_{\mathrm{A}(u)} = \Delta r_{\mathrm{B}(u)} = 22$ μm and $\Delta r_{\mathrm{A}(l)} = \Delta r_{\mathrm{B}(l)} = -22$ μm), the follower arm lengths may have tolerance amounts of $\pm\Delta l_{\mathrm{A}} = \pm\Delta l_{\mathrm{B}} = \pm 19$ μm, the radius errors of the follower rollers, $\Delta r_{f\mathrm{C}}$ and $\Delta r_{f\mathrm{D}}$, may have tolerance amounts of $\pm\Delta r_{f\mathrm{C}} = \pm\Delta r_{f\mathrm{D}} = \pm 11$ μm, and the subtending angle of the follower arms may have a tolerance amount of $\pm\Delta\eta = \pm 0.022°$. Note that this work is to estimate (calculate) the cam profile deviations Δr_{A} and Δr_{B} of being inspected ones. Therefore, for a pair of master conjugate cams and a conjugation measuring fixture constructed according to the presented method, all constant design parameters as well as the master cam profiles should have been precisely measured. Accordingly, the profile errors of the master cams, $\Delta r_{\mathrm{A}(m),\mathrm{mea}}(\theta)$ and $\Delta r_{\mathrm{B}(m),\mathrm{mea}}(\theta)$, and the five constant deviations Δl_{A}, Δl_{B}, $\Delta r_{f\mathrm{C}}$, $\Delta r_{f\mathrm{D}}$ and $\Delta\eta$ may be assumed to be known, and then the magnitudes of center distance deviations Δf_{rf}, Δf_{l} and Δf_{η} can be evaluated by using Eqs. (15)-(17), respectively, before the examination of inspected cams.

In this example, $\Delta l_{\mathrm{A}} = \Delta l_{\mathrm{B}} = 19$ μm, $\Delta r_{f\mathrm{C}} = \Delta r_{f\mathrm{D}} = 11$ μm, and $\Delta\eta = 0.022°$ are assumed. The master cams $\mathrm{A}_{(m)}$ and $\mathrm{B}_{(m)}$ are assumed to have variable profile deviations with the following

forms: $\Delta r_{A(m),mea}(\theta)$ = (18.5 + 3.5sinθ) μm and $\Delta r_{B(m),mea}(\theta)$ = (17.5 + 4.5cos2θ) μm. Then, the measured center distance variation $\Delta f_{mea}(\theta)$ caused by a pair of assembled conjugate cams consisting of a master cam and a being inspected one (either a pair of cams A and $B_{(m)}$ or the other pair of cams $A_{(m)}$ and B) is considered to have an invariant value of 22 μm, which is the corresponding value of tolerance grade IT6 of the theoretical center distance f, when the cams rotate a complete revolution. Figure 5 shows some evaluated results of this example,

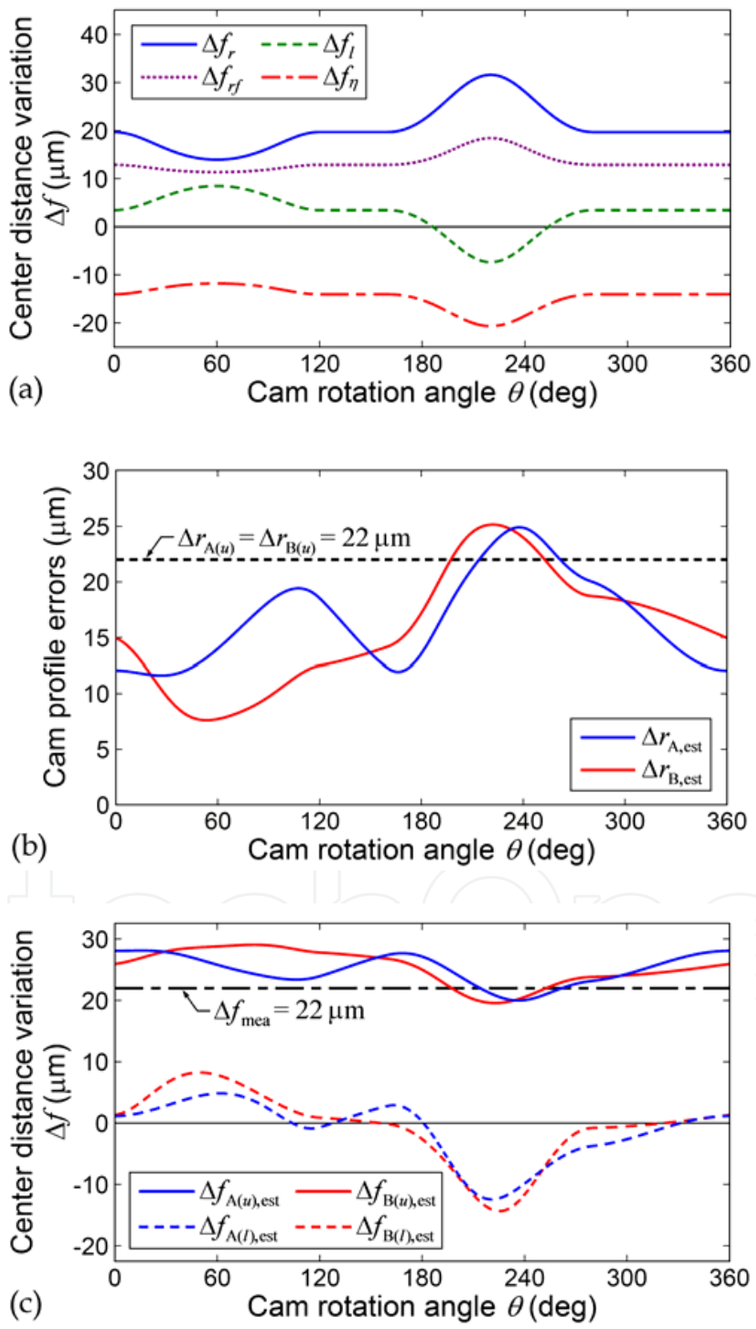

Fig. 5. Evaluated results of a simulated example

while their extreme values are also listed in Table 1. The calculated center distance variations with respect to the cam rotation angle θ are shown in Fig. 5(a), in which, Δf_{rf}, Δf_l and Δf_η are calculated by using Eqs. (15)-(17), respectively, while Δf_r is calculated by using Eq. (19). In this case, the extreme values of Δf_l and Δf_{rf} are slighter than those of Δf_r and Δf_η, while Δf_r, Δf_{rf} and Δf_η have similar variation trends if their signs are ignored. Figure 5(b) shows the estimated cam profile errors, $\Delta r_{A,est}$ and $\Delta r_{B,est}$, with respect to the cam rotation angle θ, in which, $\Delta r_{A,est}$ is calculated by using Eq. (20) with the information of $\Delta r_{B(m),mea}(\theta)$ = (17.5 + 4.5cos2θ) μm and $\Delta f_{mea}(\theta)$ = 22 μm, while $\Delta r_{B,est}$ is calculated by using Eq. (21) with the information of $\Delta r_{A(m),mea}(\theta)$ = (18.5 + 3.5sinθ) μm and $\Delta f_{mea}(\theta)$ = 22 μm. It can be seen that $\Delta r_{A,est}$ ranges between 11.62 and 24.9 μm, and $\Delta r_{B,est}$ ranges between 7.62 and 25.15 μm. Apparently, when θ = 213.97° ~ 261.78°, $\Delta r_{A,est}$ exceeds its specified upper bound $\Delta r_{A(u)}$ (= 22 μm), and when θ = 197.36° ~ 252.63°, $\Delta r_{B,est}$ also exceeds its specified upper bound $\Delta r_{B(u)}$ (= 22 μm). Such situations can also be judged through the results shown in Fig. 5(c), in which, the magnitude of Δf_{mea} (= 22 μm) is out of the range between $\Delta f_{A(l),est}$ ~ $\Delta f_{A(u),est}$ when θ = 213.97° ~ 261.78° and also out of the range between $\Delta f_{B(l),est}$ ~ $\Delta f_{B(u),est}$ when θ = 197.36° ~ 252.63°. As a result, both cams A and B in this example are partially unqualified and whose profile errors can be estimated and examined by means of the inverse conjugate variation analysis procedure.

Cam angle	Extreme value	Cam angle	Extreme value
θ = 15.6°	$(\Delta f_{A(u),est})_{max}$ = 28.14 μm	θ = 219.99°	$(\Delta f_r)_{max}$ = 31.6 μm
θ = 26.52°	$(\Delta r_{A,est})_{min}$ = 11.62 μm	θ = 219.99°	$(\Delta f_\eta)_{min}$ = −20.67 μm
θ = 49.62°	$(\Delta f_{B(l),est})_{max}$ = 8.25 μm	θ = 220°	$(\Delta f_l)_{min}$ = −7.37 μm
θ = 53.33°	$(\Delta r_{B,est})_{min}$ = 7.62 μm	θ = 220°	$(\Delta f_{rf})_{max}$ = 18.44 μm
θ = 59.92°	$(\Delta f_\eta)_{max}$ = −11.79 μm	θ = 220.75°	$(\Delta f_{A(l),est})_{min}$ = −12.43 μm
θ = 59.97°	$(\Delta f_r)_{min}$ = 13.95 μm	θ = 222.03°	$(\Delta r_{B,est})_{max}$ = 25.15 μm
θ = 59.98°	$(\Delta f_l)_{max}$ = 8.49 μm	θ = 222.78°	$(\Delta f_{B(u),est})_{min}$ = 19.58 μm
θ = 59.99°	$(\Delta f_{rf})_{min}$ = 11.35 μm	θ = 225.28°	$(\Delta f_{B(l),est})_{min}$ = −14.35 μm
θ = 62.09°	$(\Delta f_{A(l),est})_{max}$ = 4.84 μm	θ = 236.41°	$(\Delta f_{A(u),est})_{min}$ = 19.99 μm
θ = 81.65°	$(\Delta f_{B(u),est})_{max}$ = 29.08 μm	θ = 237.72°	$(\Delta r_{A,est})_{max}$ = 24.9 μm

Table 1. Extreme values of a simulated example

4. Experimental details

In order to test the feasibility and effectiveness of the presented method, an experiment meant to examine profile errors of a pair of machined conjugate cams was conducted.

4.1 Experimental apparatus

An assembled conjugate cam mechanism, whose center distance between the cam and follower pivots is variable, had been designed and built for experimental work. The built mechanism is shown in Fig. 6, which was the identical one used for the experiment of measuring the center distance variation to verify the theoretical derivation results of the conjugate variation analysis (Chang et al., 2009). The specified design parameters of this built mechanism are identical to those of the cam system illustrated in Sub-section 3.2. The conjugate cams, identical to those used for experiments conducted in previous studies

(Chang et al., 2008; Chang and Wu, 2008; Chang et al., 2009), were made of stainless steel JIS SUS304/AISI 304. Both cams had the same thickness of 12 mm and whose profiles were manufactured by a computer numerical control (CNC) electro-discharge wire-cutting (EDWC) machine. In order to make the center distance variation large enough to be easily sensed and read in the experiment, both cams had been specified to have a radial-dimension tolerance of ±220 μm (i.e., $\Delta r_{A(u)} = \Delta r_{B(u)} = 220$ μm and $\Delta r_{A(l)} = \Delta r_{B(l)} = -220$ μm in this case), a considerably large tolerance grade of IT11.

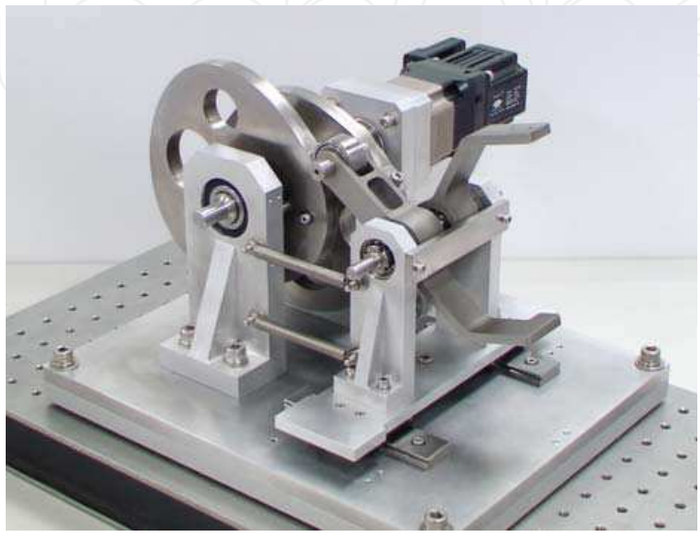

Fig. 6. Built assembled conjugate cams with measuring fixture

The experimental apparatus and instrumentation are schematically shown in Fig. 7. To drive the built conjugate cam mechanism, an Animatics SM2315D 0.13 kW DC servomotor coupled with an Apex Dynamics AB060-S1-P1 gear reducer with a reduction ratio of 9:1 were used. The servomotor was powered by a DC power supply. A personal computer was prepared to control the servomotor through a communication cable (Animatics CBLSM1) connecting the servomotor and one RS-232 port of the computer. A Mitutoyo ID-C112M 543-251 digimatic indicator, whose resolution and accuracy are 1 μm and ±3 μm, respectively, was employed to measure the center distance variation between the cam and follower pivots. The digital measuring data read from the digimatic indicator were inputted to the same computer by using a Mitutoyo MUX-10F Multiplexer data transfer device connecting the digimatic indicator and another RS-232 port of the computer. A Keyence FU-25/FS-V31 fiber optic sensor module, powered by the same DC power supply, was applied to identify the initial angular position for the cam rotation and also to ensure that the conjugate cams can actually return to the initial angular position in each revolution. The fiber optic sensor module beamed one end face of cam A for sensing and calibrating the initial angular position of the conjugate cams.

4.2 Experimental procedure

Before the experiment of examining the profile accuracy of assembled conjugate cams was conducted, the cam profiles had been measured by using a Giddings & Lewis Sheffield Measurement Cordax RS-25 CMM with a Renishaw touch-trigger probe (PH9 probe head and TP200 probe with a stylus for its ruby ball diameter of 2 mm) (Chang et al., 2008; Chang

and Wu, 2008), as shown in Fig. 8. The measuring time of each cam with 3600 points on the cam contour being measured had taken about 3 hours. The radial-dimension errors of the cams had then been evaluated from the coordinate measurement data by using the analytical approach proposed by Chang et al. (2008). Before the built conjugate cam mechanism had been assembled, the dimensions of the follower arms and the rollers had also been measured by using the CMM. Thus, the measured radial dimension errors of cams A and B, $\Delta r_{A,mea}(\theta)$ and $\Delta r_{B,mea}(\theta)$, the roller-radius errors of rollers C and D, Δr_{fC} and Δr_{fD}, and the errors of the arm lengths, Δl_A and Δl_B, had been obtained.

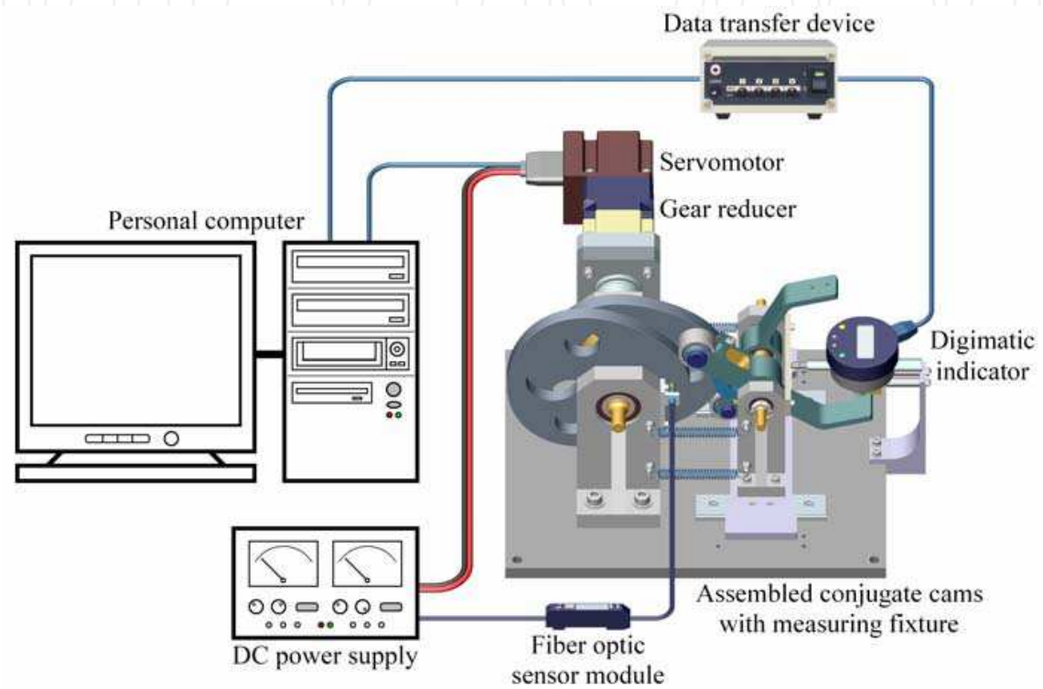

Fig. 7. Schematic of the experimental apparatus and instrumentation

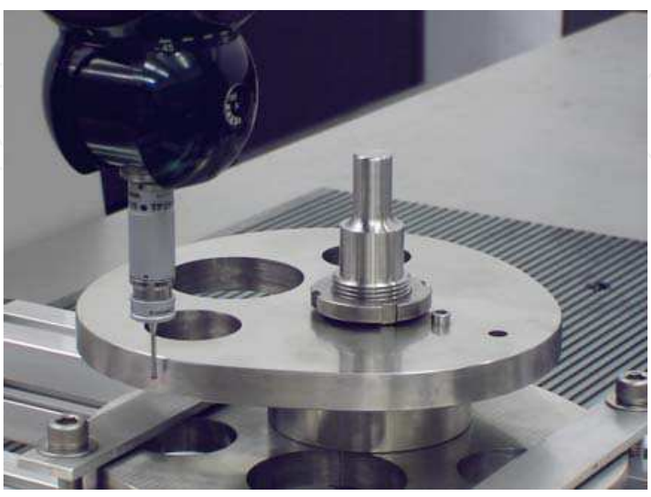

Fig. 8. Measuring the conjugate cam profiles by using a CMM

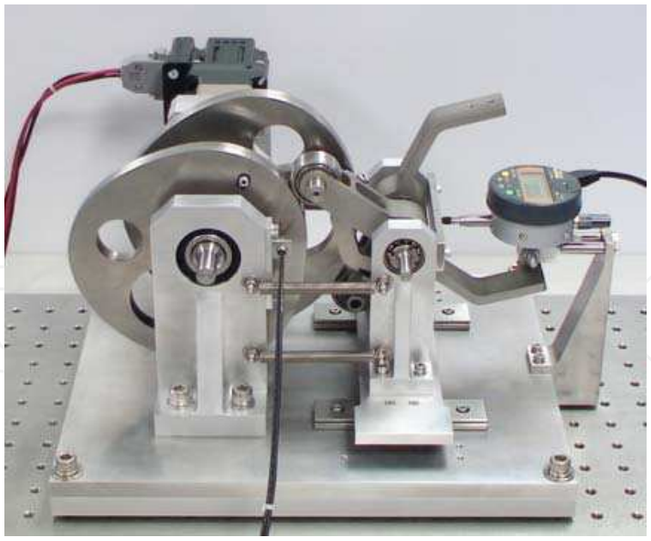

Fig. 9. Measuring the center distance variation by using a digimatic indicator

After the built conjugate cam mechanism was assembled and set for the measurement of the center distance variation in this study, as shown in Fig. 9, the fixed subtending angle between the follower arms was also measured by using the CMM to obtain the subtending angle error, $\Delta\eta$. During the measurement of the center distance variation, the conjugate cams rotated continuously with a constant angular velocity of 4 rev/hour (≈ 0.0667 rev/min ≈ 0.007 rad/sec) for 10 revolutions, while the data sampling rate was set to 5 Hz; the measuring time of the center distance variations for each revolution took 15 minutes. Ten data sets of 4500 values of the motion variations of the digimatic indicator for each cam revolution were recorded. For each revolution, 3600 interpolated values of the indicator readings corresponding to the cam angles with an equal interval of 0.1° based on the original 4500 measured values were calculated by using linear interpolation. Then, the 10 sets of the interpolated indicator reading data were obtained as the interpolated center distance variations. The averages of the interpolated center distance variations with respect to each corresponding cam rotation angle were calculated and considered as representatives of the experimental data function of angle θ, $\Delta f_{mea}(\theta)$.

The experimental data of $\Delta f_{mea}(\theta)$, $\Delta r_{A,mea}(\theta)$ and $\Delta r_{B,mea}(\theta)$ were then adopted for examining the cam profile error with the use of the presented method. For the profile error examination of cam A, data of $\Delta f_{mea}(\theta)$ and $\Delta r_{B,mea}(\theta)$ were adopted to calculate $\Delta r_{A,est}(\theta)$ by using Eq. (20). Likewise, for the profile error examination of cam B, data of $\Delta f_{mea}(\theta)$ and $\Delta r_{A,mea}(\theta)$ were adopted to calculate $\Delta r_{B,est}(\theta)$ by using Eq. (21).

5. Results and discussion

The actual dimensions of the constant parameters (i.e., l_A, l_B, r_{fC}, r_{fD} and η) and their corresponding errors in the built mechanism are listed in Table 2. [Note that the subtending angle error $\Delta\eta$ (= 0.275°) in the experiment was about 95.8 percent of that in previous study (Chang et al., 2009) because of the reassembling of the follower subassembly of the built mechanism; while the other four errors remained identical to their previous ones.] The measured cam profile errors by using a CMM (Chang et al., 2008; Chang and Wu, 2008) are

shown in Fig. 10. By using Eqs. (14)-(17) with the error terms in Table 2 and Fig. 10 being involved, the evaluated center distance variations for the experiment, Δf_r caused by $\Delta r_{A,mea}$ and $\Delta r_{B,mea}$, Δf_{rf} caused by Δr_{fC} and Δr_{fC}, Δf_l caused by Δl_A and Δl_B, and Δf_η caused by $\Delta\eta$, are shown in Fig. 11. Extreme values of related functions shown in Figs. 10 and 11 are also listed in Table 3. In Fig. 10, it can be seen that the magnitude of $\Delta r_{A,mea}$ exceeded its upper bound of $\Delta r_{A(u)}$ = 220 μm at about θ = 80° ~ 110°; while the magnitude of $\Delta r_{B,mea}$ fell within the range of its specified tolerance. Figure 11 shows that the magnitudes and variation ranges of Δf_r and Δf_η were much greater than those of Δf_{rf} and Δf_l. Thus, the cam profile errors, $\Delta r_{A,mea}$ and $\Delta r_{B,mea}$, and the subtending angle error, Δf_η, mainly dominated the trend of the overall center distance variation, Δf_{est} (= $\Delta f_r + \Delta f_{rf} + \Delta f_l + \Delta f_\eta$), calculated by using Eq. (18).

Parameter	Nominal value	Actual value (in average)	Error (in average)
l_A	66 mm	65.984 mm	16 μm
l_B	66 mm	65.932 mm	−68 μm
r_{fC}	16 mm	15.989 mm	−11 μm
r_{fD}	16 mm	15.990 mm	−10 μm
η	100°	100.275°	0.275° (≈ 0.00479 rad)

Table 2. Nominal and actual values of the constant parameters

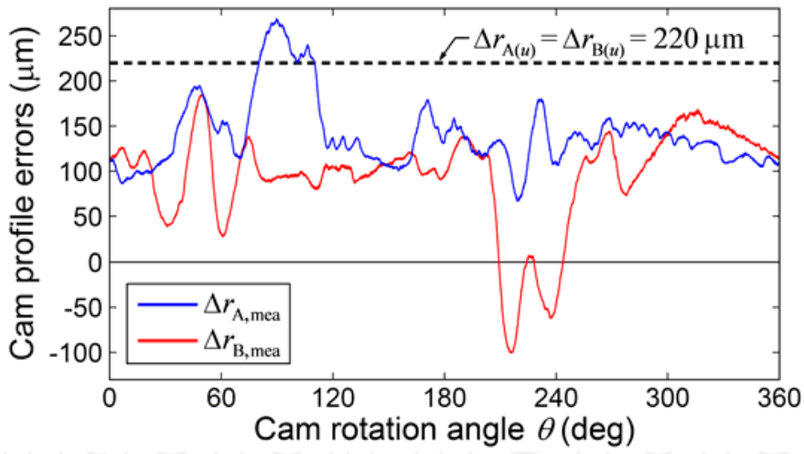

Fig. 10. Measured cam profile errors by using a CMM (Chang et al., 2008; Chang and Wu, 2008)

Figure 12 shows the measured and estimated results of the experiment. The measured and estimated center distance variations, Δf_{mea} and Δf_{est}, and their difference ($\Delta f_{est} - \Delta f_{mea}$) are shown in Fig. 12(a). The estimated and measured profile errors of cam A, $\Delta r_{A,est}$ and $\Delta r_{A,mea}$, and their difference ($\Delta r_{A,est} - \Delta r_{A,mea}$) are shown in Fig. 12(b), while the estimated and measured profile errors of cam B, $\Delta r_{B,est}$ and $\Delta r_{B,mea}$, and their difference ($\Delta r_{B,est} - \Delta r_{B,mea}$) are shown in Fig. 12(c). Extreme values and root-mean-square values of related functions shown in the figure are also listed in Tables 3 and 4, respectively. As shown in Fig. 12(a), Δf_{mea} and Δf_{est} were very close to each other, while their difference ($\Delta f_{est} - \Delta f_{mea}$), once again shown in Fig. 13(a) for clarity of illustration, ranged between −7.70 and 6.91 μm and had a root-mean-

square value of 2.75 μm. Considering that Δf_{mea} ranged between −264.59 and 5.41 μm and had a root-mean-square value of 80.85 μm, the statistically relative deviation between Δf_{mea} and Δf_{est} was evaluated as 3.4% [= (2.75/80.85) ×100%]. Such results implied well agreement between the measured results and the estimated ones.

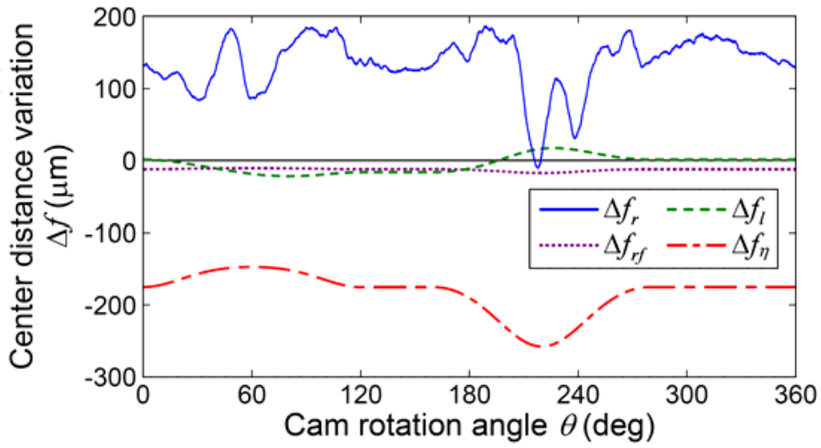

Fig. 11. Evaluated center distance variations for the experiment

Cam angle	Extreme value	Cam angle	Extreme value
θ = 45.6°	$(\Delta f_{B(l),est})_{max}$ = −175.18 μm	θ = 216.4°	$(\Delta f_{A(u),est})_{min}$ = −165.5 μm
θ = 48.4°	$(\Delta f_{est})_{max}$ = 9.31 μm	θ = 216.4°	$(\Delta f_{A(l),est})_{min}$ = −504.35 μm
θ = 48.7°	$(\Delta f_{mea})_{max}$ = 5.41 μm	θ = 217.8°	$(\Delta f_r)_{min}$ = −11.25 μm
θ = 49.4°	$(\Delta r_{B,est})_{max}$ = 180.51 μm	θ = 217.8°	$(\Delta f_{est})_{min}$ = −270.79 μm
θ = 49.7°	$(\Delta r_{B,mea})_{max}$ = 185.12 μm	θ = 218.2°	$(\Delta f_{mea})_{min}$ = −264.59 μm
θ = 49.7°	$(\Delta f_{A(l),est})_{max}$ = −199.43 μm	θ = 219.3°	$(\Delta r_{A,mea})_{min}$ = 66.95 μm
θ = 59.9°	$(\Delta f_\eta)_{max}$ = −147.14 μm	θ = 219.3°	$(\Delta f_{B(u),est})_{min}$ = −40.56 μm
θ = 61.7°	$(\Delta r_{A,est} - \Delta r_{A,mea})_{max}$ = 13.95 μm	θ = 219.3°	$(\Delta f_{B(l),est})_{min}$ = −375.73 μm
θ = 61.7°	$(\Delta r_{B,est} - \Delta r_{B,mea})_{max}$ = 13.75 μm	θ = 219.9°	$(\Delta f_{rf})_{min}$ = −17.6 μm
θ = 62.4°	$(\Delta f_{rf})_{max}$ = −10.84 μm	θ = 220°	$(\Delta f_\eta)_{min}$ = −257.89 μm
θ = 80.7°	$(\Delta f_l)_{min}$ = −22 μm	θ = 220.2°	$(\Delta r_{A,est})_{min}$ = 69.47 μm
θ = 89.2°	$(\Delta r_{A,est})_{max}$ = 260.94 μm	θ = 223.7°	$(u_f)_{max}$ = 3.7 μm
θ = 89.6°	$(\Delta r_{A,mea})_{max}$ = 268.89 μm	θ = 226.6°	$(\Delta f_l)_{max}$ = 17.28 μm
θ = 90°	$(\Delta f_{B(u),est})_{max}$ = 66.86 μm	θ = 279.6°	$(u_f)_{min}$ = 0.43 μm
θ = 179.9°	$(\Delta f_{est} - \Delta f_{mea})_{min}$ = −7.7 μm	θ = 308.6°	$(\Delta f_{est} - \Delta f_{mea})_{max}$ = 6.91 μm
θ = 188.6°	$(\Delta f_r)_{max}$ = 187.17 μm	θ = 308.6°	$(\Delta r_{A,est} - \Delta r_{A,mea})_{min}$ = −11.29 μm
θ = 215.5°	$(\Delta r_{B,mea})_{min}$ = −100.46 μm	θ = 308.6°	$(\Delta r_{B,est} - \Delta r_{B,mea})_{min}$ = −12.36 μm
θ = 215.5°	$(\Delta r_{B,est})_{min}$ = −103.14 μm	θ = 315.9°	$(\Delta f_{A(u),est})_{max}$ = 42.38 μm

Table 3. Extreme values of the experiment

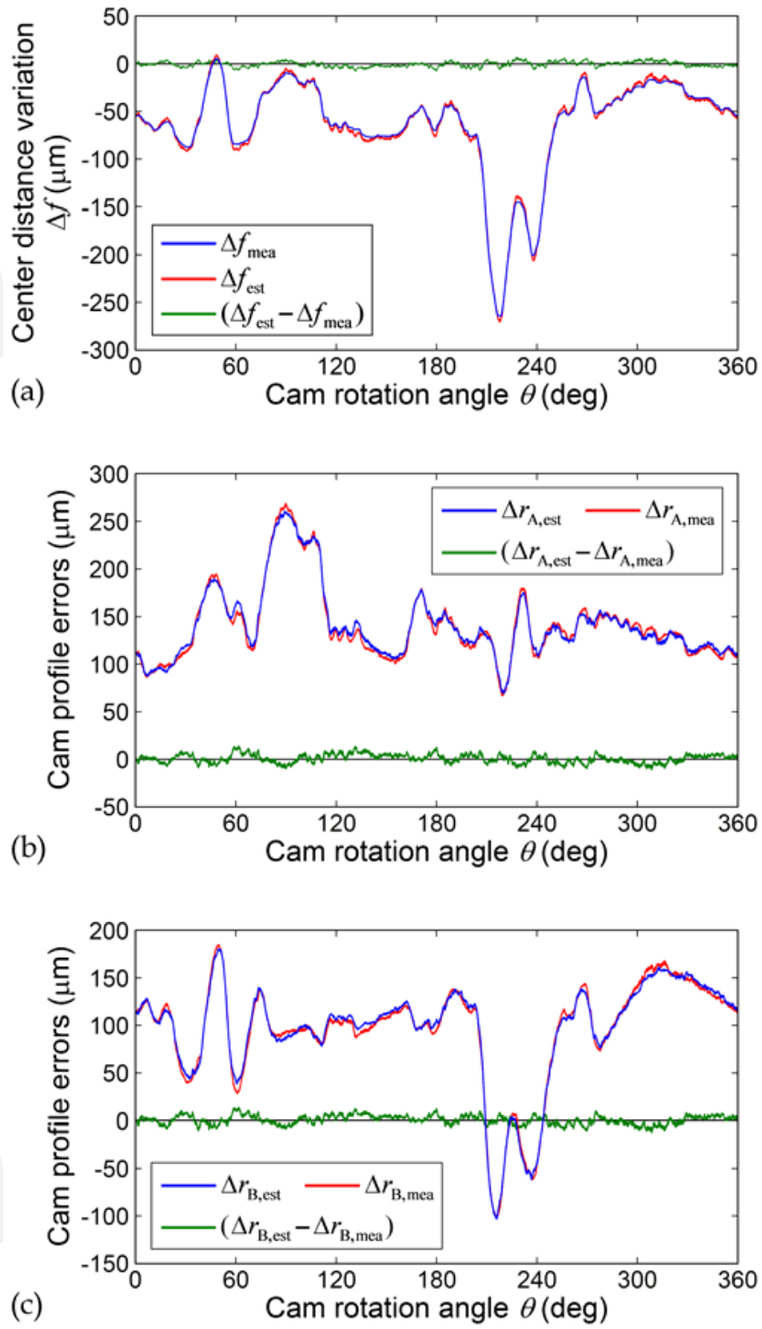

Fig. 12. Measured and estimated results of the experiment

As shown in Figs. 12(b) and 12(c), the trends and magnitudes of the estimated profile errors were well consistent with those of the measured ones. The differences between the estimated and measured profile errors are once again shown in Figs. 13(b) and 13(c) for clarity of illustration. The difference ($\Delta r_{A,est} - \Delta r_{A,mea}$) ranged between −11.29 and 13.95 μm and had a root-mean-square value of 4.68 μm. Considering that $\Delta r_{A,mea}$ ranged between 66.95 and 268.89 μm and had a root-mean-square value of 146.13 μm, the statistically relative

deviation between $\Delta r_{A,est}$ and $\Delta r_{A,mea}$ was evaluated as 3.2% [= (4.68/146.13) ×100%]. Also, the difference ($\Delta r_{B,est} - \Delta r_{B,mea}$) ranged between −12.36 and 13.75 μm and had a root-mean-square value of 4.69 μm. Considering that $\Delta r_{B,mea}$ ranged between −100.46 and 185.12 μm

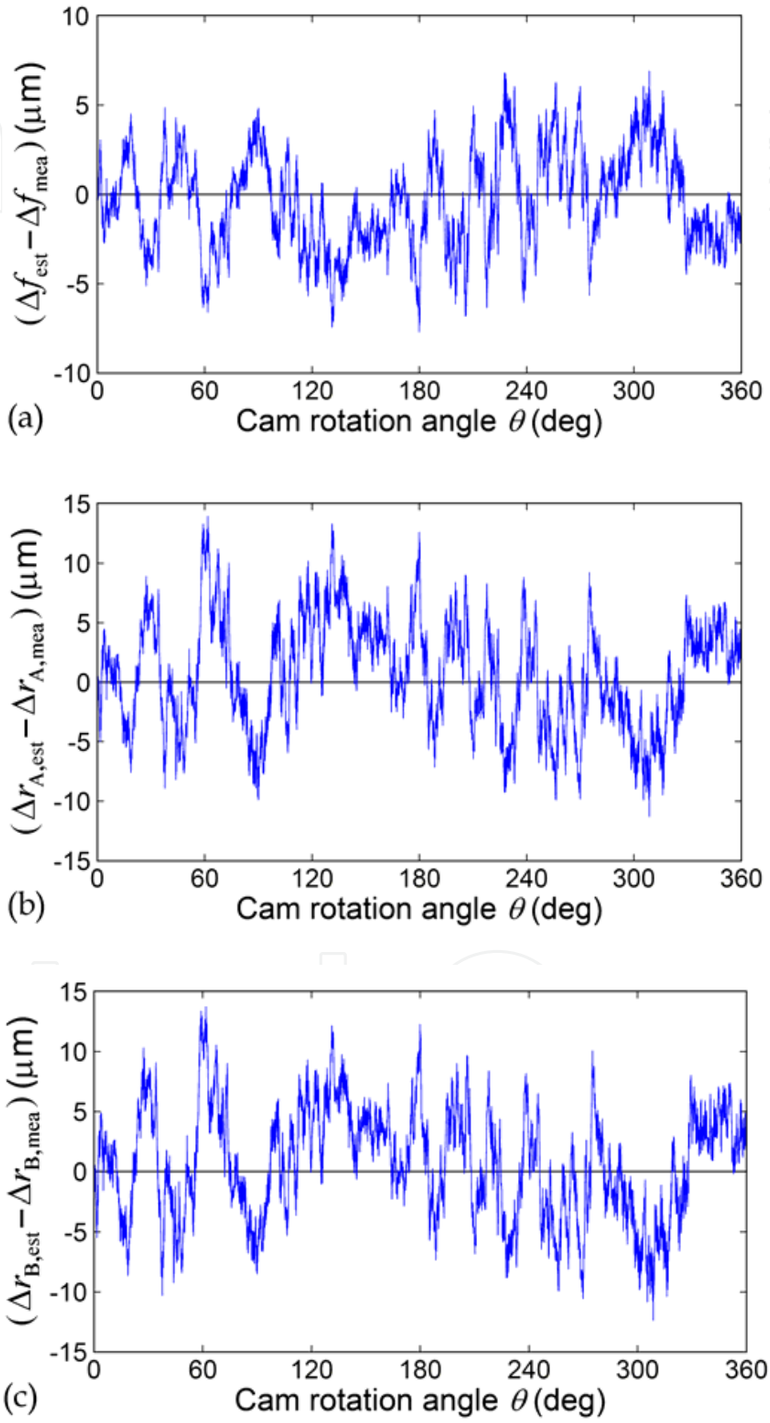

Fig. 13. Differences between the measured and estimated results

and had a root-mean-square value of 109.5 μm, the statistically relative deviation between $\Delta r_{B,est}$ and $\Delta r_{B,mea}$ was evaluated as 4.28% [= (4.69/109.5) ×100%]. Thus, from a statistical viewpoint, the differences and relative deviations in root-mean-square forms between the estimated and measured profile errors were less than 5 μm or 4.3%. Such results showed the effectiveness of the presented method for the profile error examination.

Center distance variations	Profile errors of cam A	Profile errors of cam B
$(\Delta f_{mea})_{rms}$ = 80.85 μm	$(\Delta r_{A,mea})_{rms}$ = 146.13 μm	$(\Delta r_{B,mea})_{rms}$ = 109.5 μm
$(\Delta f_{est})_{rms}$ = 81.48 μm	$(\Delta r_{A,est})_{rms}$ = 146.42 μm	$(\Delta r_{B,est})_{rms}$ = 109.8 μm
$(\Delta f_{est} - \Delta f_{mea})_{rms}$ = 2.75 μm	$(\Delta r_{A,est} - \Delta r_{A,mea})_{rms}$ = 4.68 μm	$(\Delta r_{B,est} - \Delta r_{B,mea})_{rms}$ = 4.69 μm

Table 4. Root-mean-square values of the experiment

In Fig. 13, it is found that without considering the scale, the wave of difference $(\Delta f_{est} - \Delta f_{mea})$ was upside down to the waves of their corresponding differences $(\Delta r_{A,est} - \Delta r_{A,mea})$ and $(\Delta r_{B,est} - \Delta r_{B,mea})$, respectively. In other words, the deviations between the measured and estimated center distance variations should proportionally influence the accuracy of the estimated profile errors. Figure 14 shows the uncertainty of the measured center distance variations, u_f, which is evaluated from the 10 data sets of the interpolated center distance variations through using the three-standard-deviation-band approach (Beckwith et al., 2004) with respect to each corresponding cam rotation angle. The evaluated uncertainty u_f ranged between 0.43 and 3.7 μm and had a root-mean-square value of 1.97 μm. The statistical representatives of the measured center distance variations, $\Delta f_{mea,SR}$, can be expressed as

$$\Delta f_{mea,SR} = \Delta f_{mea} \pm u_f \tag{32}$$

Thus, the upper and lower bounds of $\Delta f_{mea,SR}(\theta)$, $\Delta f_{mea,SR(u)}(\theta)$ and $\Delta f_{mea,SR(l)}(\theta)$, are defined as terms $[\Delta f_{mea}(\theta) + u_f(\theta)]$ and $[\Delta f_{mea}(\theta) - u_f(\theta)]$, respectively. Considering one of the worst cases, when data of $\Delta f_{mea,SR(u)}(\theta)$, $\Delta r_{A,mea}(\theta)$ and $\Delta r_{B,mea}(\theta)$ were adopted to calculate $\Delta r_{A,est}(\theta)$ and $\Delta r_{B,est}(\theta)$ by using Eqs. (20) and (21), respectively, the evaluated difference $(\Delta r_{A,est} - \Delta r_{A,mea})$ as shown in Fig. 15(a) ranged between −6.8 and 17.57 μm and had a root-mean-square value

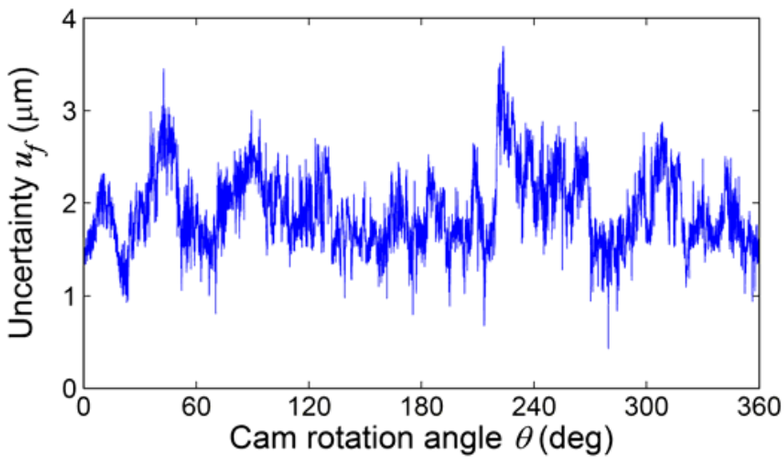

Fig. 14. Uncertainty of the measured center distance variations

of 5.97 μm, and the evaluated difference ($\Delta r_{B,est} - \Delta r_{B,mea}$) as shown in Fig. 15(b) ranged between −7.44 and 17.32 μm and had a root-mean-square value of 5.93 μm. The statistically relative deviation between $\Delta r_{A,est}$ and $\Delta r_{A,mea}$ was evaluated as 4.09% [= (5.97/146.13) ×100%], and that between $\Delta r_{B,est}$ and $\Delta r_{B,mea}$ was evaluated as 5.42% [= (5.93/109.5) ×100%]. Likewise, considering the other of the worst cases, when data of $\Delta f_{mea,SR(l)}(\theta)$, $\Delta r_{A,mea}(\theta)$ and $\Delta r_{B,mea}(\theta)$ were adopted to calculate $\Delta r_{A,est}(\theta)$ and $\Delta r_{B,est}(\theta)$ by using Eqs. (20) and (21), respectively, the evaluated difference ($\Delta r_{A,est} - \Delta r_{A,mea}$) as shown in Fig. 16(a) ranged between −15.78 and 10.32 μm and had a root-mean-square value of 5.55 μm, and the evaluated difference ($\Delta r_{B,est} - \Delta r_{B,mea}$) as shown in Fig. 16(b) ranged between −17.27 and 10.18 μm and had a root-mean-square value of 5.64 μm. The statistically relative deviation between $\Delta r_{A,est}$ and $\Delta r_{A,mea}$ was evaluated as 3.8% [= (5.55/146.13) ×100%], and that between $\Delta r_{B,est}$ and $\Delta r_{B,mea}$ was evaluated as 5.15% [= (5.64/109.5) ×100%]. In other words, when considering the worst cases, the differences and relative deviations in root-mean-square forms between the estimated and measured profile errors were still less than 6 μm or 5.5%. Therefore, the uncertainty of the measured center distance variations in this experiment should have merely slight effect on influencing the accuracy of the estimated profile errors.

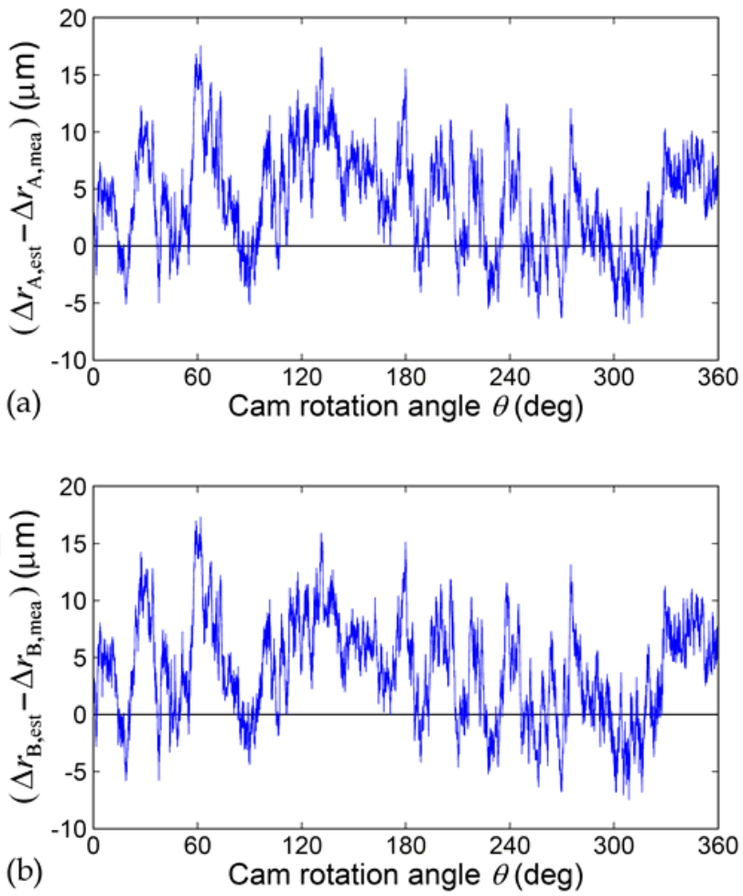

Fig. 15. Differences between the measured and estimated results evaluated by considering the upper bounds of the statistical representatives of the measured center distance variations

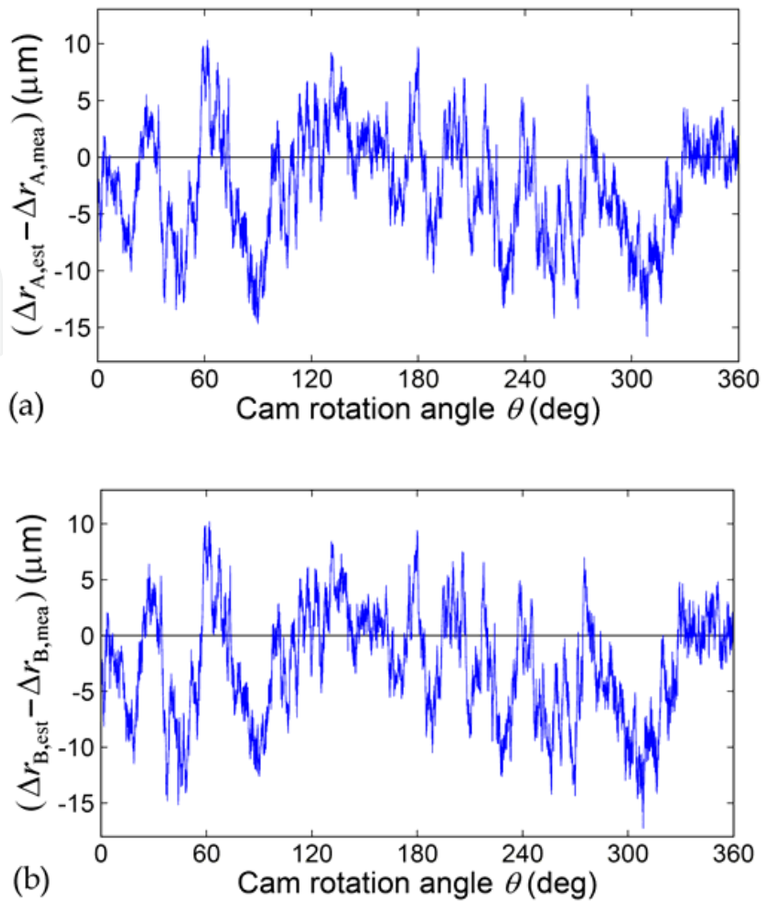

Fig. 16. Differences between the measured and estimated results evaluated by considering the lower bounds of the statistical representatives of the measured center distance variations

In addition, by applying the criteria established in Sub-section 3.1, the allowable upper and lower limits of the measured center distance variations are shown in Fig. 17, and whose extreme values are also listed in Table 3. As shown in the figure, the measured values of Δf_{mea} exceeded their allowable upper bound, $\Delta f_{A(u),est}$, when θ = 80° ~ 110° but totally fell within the range of $\Delta f_{B(l),est}$ ~ $\Delta f_{B(u),est}$. Recall from Fig. 10 that the magnitude of $\Delta r_{A,mea}$ exceeded the specified tolerance of ±220 μm at about θ = 80° ~ 110°, while the magnitude of $\Delta r_{B,mea}$ fell within the range of its specified tolerance. Obviously, the profile error evaluating results by using the established criteria agreed with the measuring results by using a CMM. As a result, the method presented in this study has been verified a feasible means for examining profile errors of assembled conjugate disk cams.

As compared with the use of a CMM to examine profile errors of conjugate disk cams that had taken 3 hours for measuring each cam, the presented method that took 15 minutes for examining each cam through the rotation of the assembled conjugate cams for 1 revolution could provide acceptable results with efficiency. Although the presented method cannot completely replace the use of CMMs, but in certain aspects it should be a more convenient and inexpensive means for the quality control in mass production of assembled conjugate disk cams.

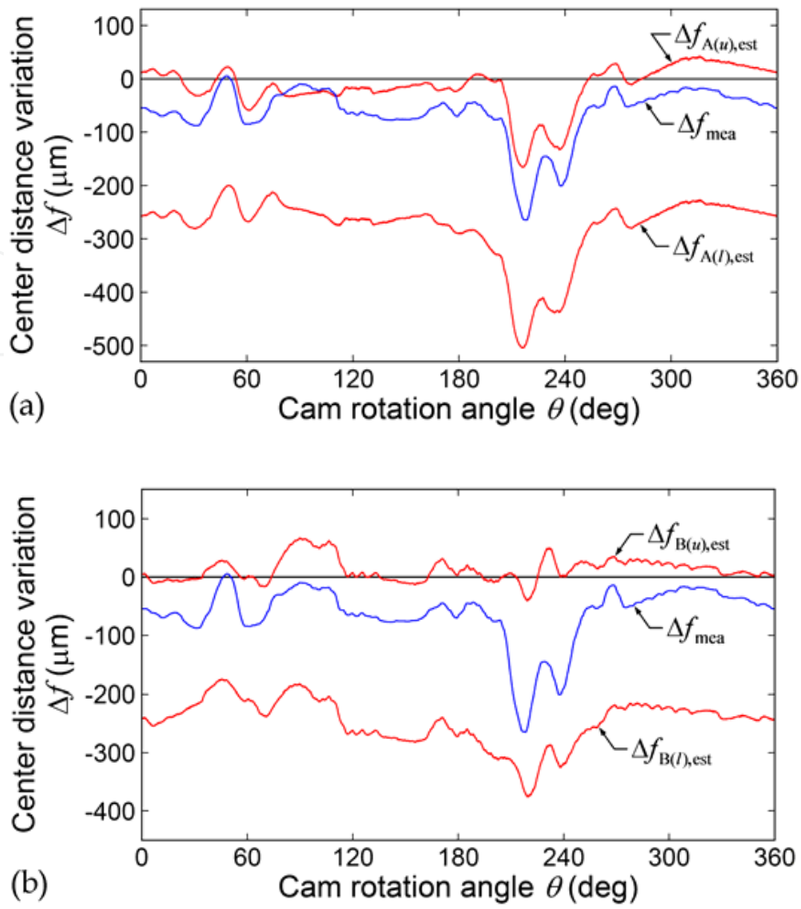

Fig. 17. Allowable upper and lower limits of the measured center distance variations

6. Conclusion

Based on combining the concepts of conjugate variation measurement and inverse conjugate variation analysis, the profile accuracy of assembled conjugate disk cams can be examined by a convenient and inexpensive manner. If a pair of master conjugate cams with known profile errors and a set of conjugation measuring fixture are available, by means of the measured center distance variations between the cam and follower pivots induced by a pair of assembled conjugate cams consisting of one master cam and the other being the inspected cam, then the profile errors of the inspected cam can be estimated with the use of the analytical equations derived in this study. Then, the accuracy of the inspected cam can be examined through the information of the measured center distance variations with the use of the criteria established in this study. An experiment meant to examine the profile errors of a pair of machined conjugate cams had been conducted. The machined conjugate cams had been examined by the presented method to compare with the measuring results obtained by using a CMM. The experimental results showed that the estimated profile errors were well consistent with those of the measured ones by using a CMM. From a statistical viewpoint, the differences and relative deviations in root-mean-square forms between the estimated and measured results of the cam profile errors were less than 6 μm

and 5.5%, respectively, even though the machined cams had been intentionally specified to have a large tolerance grade of IT11. In conclusion, the method presented in this study has been verified a feasible and efficient alternative means for examining profile errors of assembled conjugate disk cams. Therefore, the presented method could be useful for the quality control in mass production of assembled conjugate disk cams and may replace the use of expensive CMMs in certain aspects. Integrating the presented method with machine system design to develop a specialized quality control system could be possible future work.

7. Acknowledgment

The authors are grateful to the National Science Council of Taiwan for supporting this research under Grant No. NSC-95-2221-E-007-012-MY2 and Grant No. NSC-98-2221-E-007-015-MY2.

8. References

Beckwith, T.G.; Marangoni, R.D. & Lienhard V, J.H. (2004). *Mechanical Measurements* (5th edition), pp. 45-125, Pearson Education Taiwan, ISBN 986-154-022-9, Taipei, Taiwan

Chang, W.T. & Wu, L.I. (2006). Mechanical Error Analysis of Disk Cam Mechanisms with a Flat-Faced Follower. *Journal of Mechanical Science and Technology*, Vol.20, No.3, (March 2006), pp. 345-357, ISSN 1738-494X

Chang, W.T.; Wu, L.I.; Fuh, K.H. & Lin, C.C. (2008). Inspecting Profile Errors of Conjugate Disk Cams with Coordinate Measurement. *Transactions of the ASME, Journal of Manufacturing Science and Engineering*, Vol.130, No.1, (February 2008), 011009, ISSN 1087-1357

Chang, W.T. & Wu, L.I. (2008). A Simplified Method for Examining Profile Deviations of Conjugate Disk Cams. *Transactions of the ASME, Journal of Mechanical Design*, Vol.130, No.5, (May 2008), 052601, ISSN 1050-0472

Chang, W.T.; Wu, L.I. & Liu, C.H. (2009). Inspecting Profile Deviations of Conjugate Disk Cams by a Rapid Indirect Method. *Mechanism and Machine Theory*, Vol.44, No.8, (August 2009), pp. 1580-1594, ISSN 0094-114X

Hsieh, J.F. & Lin, P.D. (2007). Application of Homogenous Transformation Matrix to Measurement of Cam Profiles on Coordinate Measuring Machines. *International Journal of Machine Tools and Manufacture*, Vol.47, No.10, (August 2007), pp. 1593-1606, ISSN 0890-6955

Koloc, Z. & Václavík, M. (1993). *Cam Mechanisms*, pp. 411-413, Elsevier, ISBN 0-444-98664-2, New York, USA

Lin, P.D. & Hsieh, J.F. (2000). Dimension Inspection of Spatial Cams by CNC Coordinate Measuring Machines. *Transactions of the ASME, Journal of Manufacturing Science and Engineering*, Vol.122, No.1, (February 2000), pp. 149-157, ISSN 1087-1357

Norton, R.L. (2009). *Cam Design and Manufacturing Handbook* (2nd edition), pp. 27-30, pp. 433-440, Industrial Press, ISBN 978-0-8311-3367-2, New York, USA

Qiu, H.; Li, Y.; Cheng, K. & Li, Y. (2000). A Practical Evaluation Approach towards Form Deviation for Two-Dimensional Contours Based on Coordinate Measurement Data. *International Journal of Machine Tools and Manufacture*, Vol.40, No.2, (January 2000), pp. 259-275, ISSN 0890-6955

Qiu, H.; Li, Y.B.; Cheng, K.; Li, Y. & Wang, J. (2000). A Study on an Evaluation Method for Form Deviations of 2D Contours from Coordinate Measurement. *The International Journal of Advanced Manufacturing Technology*, Vol.16, No.6, (May 2000), pp. 413-423, ISSN 0268-3768

Qiu, H.; Cheng, K.; Li, Y.; Li, Y. & Wang, J. (2000). An Approach to Form Deviation Evaluation for CMM Measurement of 2D Curve Contours. *Journal of Materials Processing Technology*, Vol.107, No.1-3, (November 2000), pp. 119-126, ISSN 0924-0136

Rothbart, H.A. (Ed.) (2004). *Cam Design Handbook*, pp. 8-9, pp. 44-46, McGraw-Hill, ISBN 0-07-137757-3, New York, USA

Wu, L.I. (2003). Calculating Conjugate Cam Profiles by Vector Equations. *Proceedings of the Institution of Mechanical Engineers, Part C: Journal of Mechanical Engineering Science*, Vol.217, No.10, (October 2003), pp. 1117-1123, ISSN 0954-4062

Wu, L.I. & Chang, W.T. (2005). Analysis of Mechanical Errors in Disc Cam Mechanisms. *Proceedings of the Institution of Mechanical Engineers, Part C: Journal of Mechanical Engineering Science*, Vol.219, No.2, (February 2005), pp. 209-224, ISSN 0954-4062

Wide Spectra of Quality Control

Edited by Dr. Isin Akyar

ISBN 978-953-307-683-6
Hard cover, 532 pages
Publisher InTech
Published online 07, July, 2011
Published in print edition July, 2011

Quality control is a standard which certainly has become a style of living. With the improvement of technology every day, we meet new and complicated devices and methods in different fields. Quality control explains the directed use of testing to measure the achievement of a specific standard. It is the process, procedures and authority used to accept or reject all components, drug product containers, closures, in-process materials, packaging material, labeling and drug products, and the authority to review production records to assure that no errors have occurred.The quality which is supposed to be achieved is not a concept which can be controlled by easy, numerical or other means, but it is the control over the intrinsic quality of a test facility and its studies. The aim of this book is to share useful and practical knowledge about quality control in several fields with the people who want to improve their knowledge.

InTech Europe
University Campus STeP Ri
Slavka Krautzeka 83/A
51000 Rijeka, Croatia
Phone: +385 (51) 770 447
Fax: +385 (51) 686 166
www.intechopen.com

InTech China
Unit 405, Office Block, Hotel Equatorial Shanghai
No.65, Yan An Road (West), Shanghai, 200040, China
中国上海市延安西路65号上海国际贵都大饭店办公楼405单元
Phone: +86-21-62489820
Fax: +86-21-62489821

IntechOpen